Since January 2020 Elsevier has created a COVID-19 resource centre with free information in English and Mandarin on the novel coronavirus COVID-19. The COVID-19 resource centre is hosted on Elsevier Connect, the company's public news and information website.

Biosensors and Bioelectronics 42 (2013) 236–241

Contents lists available at SciVerse ScienceDirect

Biosensors and Bioelectronics

journal homepage: www.elsevier.com/locate/bios

Colorimetric viral detection based on sialic acid stabilized gold nanoparticles

Changwon Lee [a], Marsha A. Gaston [b], Alison A. Weiss [b], Peng Zhang [a,*]

[a] Department of Chemistry, Biochemistry & Microbiology, University of Cincinnati, Cincinnati, OH 45221, United States
[b] Department of Molecular Genetics, Biochemistry & Microbiology, University of Cincinnati, Cincinnati, OH 45221, United States

ARTICLE INFO

Article history:
Received 26 July 2012
Received in revised form
5 October 2012
Accepted 19 October 2012
Available online 6 November 2012

Keywords:
Sialic acid
Au nanoparticle
Viral detection
Colorimetric measurement

ABSTRACT

Sialic acid reduced and stabilized gold nanoparticles ($d=20.1\pm1.8$ nm) were synthesized by a simple one-pot, green method without chemically modifying sialic acid for colorimetric detection of influenza virus. The gold nanoparticles showed target-specific aggregation with viral particles via hemagglutinin–sialic acid binding. A linear correlation was observed between the change in optical density and dilution of chemically inactivated influenza B/Victoria and influenza B/Yamagata. Virus dilution (hemagglutination assay titer, 512) of 0.156 vol% was readily detected. The upper limit of the linearity can be extended with the use of more sialic acid–gold nanoparticles.

1. Introduction

Over 75% of all acute morbidities in developed countries are associated with acute respiratory diseases and 80% of these infections are viral (Mahony, 2008). Of these viral infections, influenza virus causes approximately 200,000 hospitalizations and 36,000 deaths per year in the United States alone (Thompson et al., 2004). Young children, the elderly, and those with weakened immune systems are at increased risk.

Surveillance is an important facet of influenza control. Rapid, accurate diagnostic tests for influenza can direct efforts for appropriate treatment of infected individuals and public health measures to prevent spread. For example, identification and isolation of infected individuals has been shown to prevent disease and be cost effective in the setting of pediatric hospitals and nursing homes (Salgado et al., 2002). It is important to note that viral shedding occurs before symptoms appear, and asymptomatic individuals are an important source of infection. Tests which identify such carriers would be very beneficial. Thus, early detection of virus infection in human and animals is of great importance.

Influenza diagnostic methods, including their advantages and disadvantages were recently reviewed in Landry (2011). Highly sensitive diagnostic tests for influenza virus (such as PCR-based tests) require a high level of technical expertise, expensive reagents, and more time than is useful for diagnostic purposes. Rapid tests, based on antibody-mediated detection of viral antigens, can display poor sensitivity. These limitations make new influenza detection methodologies desirable.

Sialic acid, present on the surface of lung epithelial cells, is recognized as the primary binding determinant for influenza virus. Hemagglutinin is a surface protein on various viral species that can bind to sialic acid on targeted cell surface (Sauter et al., 1992). The binding of viral proteins to sialic acid has been studied for different pathogenic viruses, such as influenza virus (Sauter et al., 1992; Varghese et al., 1997; Weis et al., 1988), human parainfluenza virus (Suzuki et al., 2001), human coronavirus (Vlasak et al., 1988; Kunkel and Herrler, 1993) and a specific serotype of rhinovirus (Uncapher et al., 1991). Based on the binding capability of sialic acid to certain viruses, it is possible to design a colorimetric sensor for detecting virus using self-reporting plasmonic nanoparticles, which display plasmon shift upon binding to viral particles. Such a quick and user-friendly detection method based on the binding between the influenza virus envelope protein hemagglutinin and sialic acid that is capable of effectively identifying individuals or animals infected with virus can help with early therapeutic intervention and reduce the spread of infection.

Surface plasmon resonance of metallic nanoparticles strongly relies on the size and shape of individual nanoparticles and interparticle distance (Zhong et al., 2004). The assembly of metallic nanoparticles usually results in a red shift of the plasmonic peak and has been well adopted into various detection schemes with specific targeting elements displayed on the nanoparticle surface for many targets, such as polynucleotides (Elghanian et al., 1997; Storhoff et al., 2004), enzymes (Pavlov et al., 2004), cells (Medley et al., 2008), and heavy metals (Darbha et al., 2008). Still, there have

* Corresponding author. Tel.: +1 513 556 9222.
E-mail address: peng.zhang@uc.edu (P. Zhang).

0956-5663/$ - see front matter © 2012 Elsevier B.V. All rights reserved.
http://dx.doi.org/10.1016/j.bios.2012.10.067

yet to be reported for actual virus detection. Herein we report the development of sialic acid stabilized gold nanoparticles (SA-AuNPs) through a simple one-pot synthesis and their use in the detection of two influenza virus type B, subtypes Victoria and Yamagata. In our method, sialic acid was used without any chemical modification which is often time consuming and costly, such as previously reported sialic acid functionalized gold nanoparticles (Niikura et al., 2009; Papp et al., 2010).

2. Materials and methods

2.1. Chemicals and materials

N-acetylneuraminic acid (a predominant form of sialic acid, SA), sodium hydroxide, chloroauric acid ($HAuCl_4$), and β-propiolactone were purchased from Sigma-Aldrich (St. Louis, MO). Influenza B/Victoria and influenza B/Yamagata were provided by the Laboratory for Specialized Clinical Studies at Cincinnati Children's Hospital Medical Center. Heat-inactivated fetal bovine serum (FBS) and Dulbecco's Modified Eagle Media (DMEM) were purchased from Gibco by Life Technologies (Grand Island, NY).

2.2. SA-AuNP synthesis

Ten mL of 1.25 mM sialic acid was prepared in DI water and mixed with 250 μL of 0.02 M $HAuCl_4$ followed by the addition of 50 μL 1 M NaOH. The mixture was then stirred and heated for 80 °C at 1200 rpm for 15 min. The color of the solution changed from yellow to a dark red wine. After the solution was cooled to room temperature, the gold nanoparticles were washed twice by centrifugation at 10,000 rpm using a bench-top centrifuge (Eppendorf 5424) for 20 min. After the centrifugation, supernatant was removed and the dark red pellet was suspended in DI water and stored until further use.

2.3. Gelatin-AuNP synthesis

Gelatin was dissolved in 20 mL of DI water (0.1 wt%) followed by the addition of 200 μL of 1 M NaOH solution and 250 μL of 20 mM $HAuCl_4 \cdot 4H_2O$ solution. Then the mixture was stirred at 700 rpm with magnetic stirring bar at 70 °C for 48 h. The color of the solution became a dark red wine. The product was purified by centrifugation twice at 15,000 rpm for 30 min. The purified gelatin-stabilized gold nanoparticles (Gelatin-AuNPs) were redispersed in DI water and stored for later use.

2.4. Influenza virus titer and inactivation

The number of viral particles was estimated from HA titer (Killian, 2008); for influenza B/Victoria (hemagglutination assay (HA) titer 512) this was calculated at approximately 1×10^9–1×10^{10} viral particles/mL and influenza B/Yamagata (HA titer 256) 5×10^9–5×10^{10} viral particles/mL. Virus was inactivated after incubation with a final concentration of 0.05% β-propiolactone for 1 h at 37 °C. Inactivated virus was stored at −20 °C.

2.5. Colorimetric detection of viral particles

Five hundred μL of SA-AuNP solution was mixed with different dilutions of influenza virus solution and added to a 1-cm pathlength quartz cuvette. The cuvette was then placed in UV–vis spectrometer (USB 4000, Ocean Optics) and absorption spectra were measured every minute until a plateau was reached.

2.6. Fourier transform-infrared (FT-IR) spectroscopy

Surface functional groups of SA-AuNPs were characterized by FT-IR on an ATR cell (Nicolet 6700 FT-IR, Thermo Fisher) with sample solution drops dried on the aluminum foil.

2.7. Transmission Electron Microscopy (TEM) characterization of SA-AuNPs

SA-AuNPs were first suspended in DI water through sonication to ensure the extraction of representative dispersion volumes. A drop of suspension was then deposited on a carbon-coated copper grid (300 mesh, Electron Microscopy Sciences) and permitted to dry at room temperature. TEM images were taken on a Phillips Biotwin 12 transmission (FEI) electron microscope.

2.8. Particle size analysis

Particle size analysis was performed by a Zetatrac instrument (Microtrac) with built-in liquid sample holder. The concentration of the sample was adjusted for the optimal measurement condition. Three 30 s measurements were averaged for particle size determination.

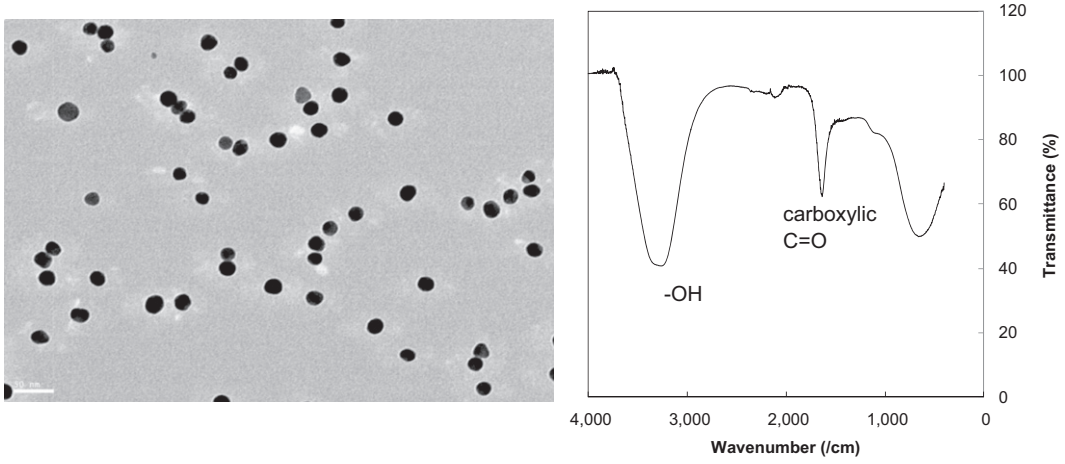

Fig. 1. Physical analysis of SA-AuNP: (A) TEM image of SA-AuNPs (scale bar is 50 nm) and (B) FT-IR analysis of SA-AuNPs.

3. Results and discussion

SA-AuNPs were synthesized in a one-pot reaction using $HAuCl_4$ as the gold source and sialic acid as both the reducing and protecting agent. The color of the solution changed from yellow to dark red wine as the reaction proceeded to completion. The SA-AuNPs were fairly monodispersed with spherical shape, as demonstrated by TEM (Fig. 1A). The average SA-AuNP size was determined to be 20.1 ± 1.8 nm after analyzing 50 particles using Adobe Photoshop software.

The concentration of the final SA-AuNPs solution was determined by the volume-density method, based on the assumption of face centered cubic (fcc) gold structure and 100% reaction yield. First, the number of gold atoms in a gold nanoparticle was calculated by the following equation

$$N = \frac{4\pi\rho r^3}{3}\frac{N_A}{M}$$

where N is the number of atoms in a gold nanoparticle, ρ is the density of fcc gold (19.3 g/cm^3), r is the radius of nanoparticle (10.05 nm), N_A is Avogadro's number and M is gold atom's atomic weight (196.97 g/mole). The calculation yielded ~250,000 gold atoms in 20.1 nm gold nanoparticles. Since the initial concentration of $HAuCl_4$ is 0.5 mM, the final SA-AuNP concentration is 2 nM when resuspended in the same volume of DI water as initially.

Sialic acid is the only compound among all starting reagents in the reaction pot that can reduce $HAuCl_4$ and stabilize the resulting AuNPs. Sialic acid contains five hydroxyl groups and one secondary amine group, all with mild capability to reduce $HAuCl_4$ and form AuNPs. This straightforward one-pot approach for synthesizing SA-AuNPs is much more efficient than previously reported methods using lab-synthesized thiolated sialic acid molecules that require multiple steps of organic synthesis and purification (Niikura et al., 2009; Papp et al., 2010). The SA-AuNPs solution is very stable in solution sitting on bench top for at least 9 months after the synthesis.

FT-IR was performed to determine the surface functional groups of the SA-AuNPs (Fig. 1B). A strong, broad band at 3000–3500 cm^{-1} corresponds to hydroxyl groups and another strong band at ~1600 cm^{-1} corresponds to the carbonyl group of carboxylic acid. Together, these data indicate the presence of sialic acid on the surface of gold nanoparticles.

The scheme of using SA-AuNPs for virus detection is shown in Fig. 2. It is known that the carboxylic group of SA is critical for the binding of hemagglutinin on the viral particles to SA on the surface of cells (Wang et al., 2007). Most of the hydroxyl and amine groups of SA-AuNPs are located at the opposite end to the carboxylic group. It is reasonable to project that the carboxylic group will face outward after SA-AuNPs are formed. The SA layer on AuNP surface prevents the aggregation of the AuNPs in solution. In the presence of viral particles, single AuNPs can attach to hemagglutinin on viral particle surface, resulting in shorter distance between AuNPs. It is expected that interaction among AuNPs would lead to a change in the absorption spectra, thus signaling the presence of viral particles.

Experimentally, absorption spectra were taken every minute after influenza B/Victoria solution of 1.25 vol% was mixed with 0.8 nM SA-AuNPs solution until each spectrum stabilized. As shown in Fig. 3A and B, the UV–vis absorption spectrum of the SA-AuNPs solution changes immediately after the addition of virus, indicating aggregation of SA-AuNPs has place. After adding dilutions of influenza B/Victoria to the SA-AuNPs solution, the OD value at 600–610 nm increases while that at 510 nm decreases over time. The increased absorbance at 600–610 nm indicates that AuNP aggregates have formed, thus decreasing the population of single AuNPs as they are converted into AuNP aggregate on the viral particle surface. The increase in absorbance at 600–610 nm is approximately 7 times that of decrease in absorbance at 510 nm, which is likely attributed to the enhanced scattering effect of aggregated AuNPs as compared to individual AuNPs.

Particle size analysis performed before and after the addition of 1.25 vol% influenza B/Victoria provided more evidences of AuNP aggregate formation. Before the addition of virus, the size distribution of the SA-AuNPs was represented as a peak at ~21 nm when measured by the Zetatrac instrument, matching well with the results from the TEM measurement (Fig. 3C). After incubating SA-AuNPs with virus, the SA-AuNPs displayed bimodal size distribution, with peaks at 28 nm and 141 nm, indicating that there are populations of both individual SA-AuNPs and virus-bound SA-AuNPs present in the solution. The size of SA-AuNP aggregates on viral particle at 141 nm correlates with the 100 nm size of a influenza B virus particle (Bouvier and Palese, 2008) (Fig. 3D).

As the stock vials of viral particles were suspended in 10% FBS containing DMEM, the specificity of this detection scheme for virus rather than media components was investigated. A control experiment was thus performed using only 10% FBS containing DMEM, where the effects of inorganic salts and the biological components, such as proteins, amino acids, vitamins, on the SA-AuNPs can be monitored. A solution containing 0.2 nM SA-AuNPs and 5 vol% of the medium was prepared and absorption spectrum was measured after 20 min (Fig. 4A). Since the absorption spectrum of the medium overlaps somewhat with the plasmonic peak area of SA-AuNPs, absorption spectrum of the medium was subtracted from that of the SA-AuNPs and medium mixture (Fig. 4A, dotted line). The corrected absorption spectrum of the SA-AuNPs in media

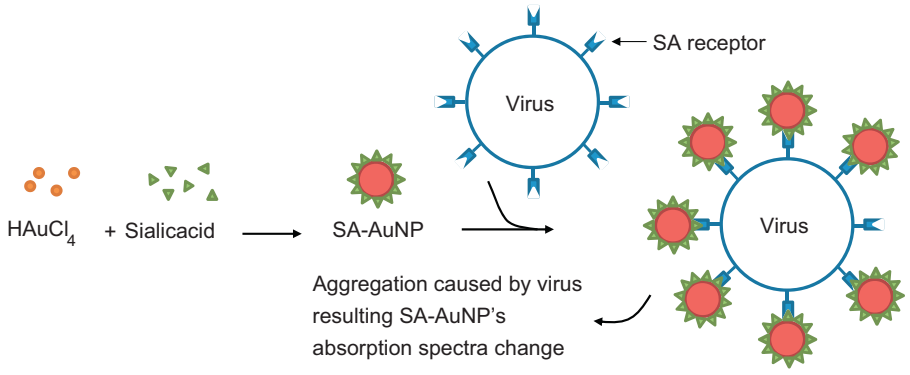

Fig. 2. Schematic of SA-AuNP synthesis and UV–vis optical detection of viral particles based on the aggregation of SA-AuNPs on the virus surface.

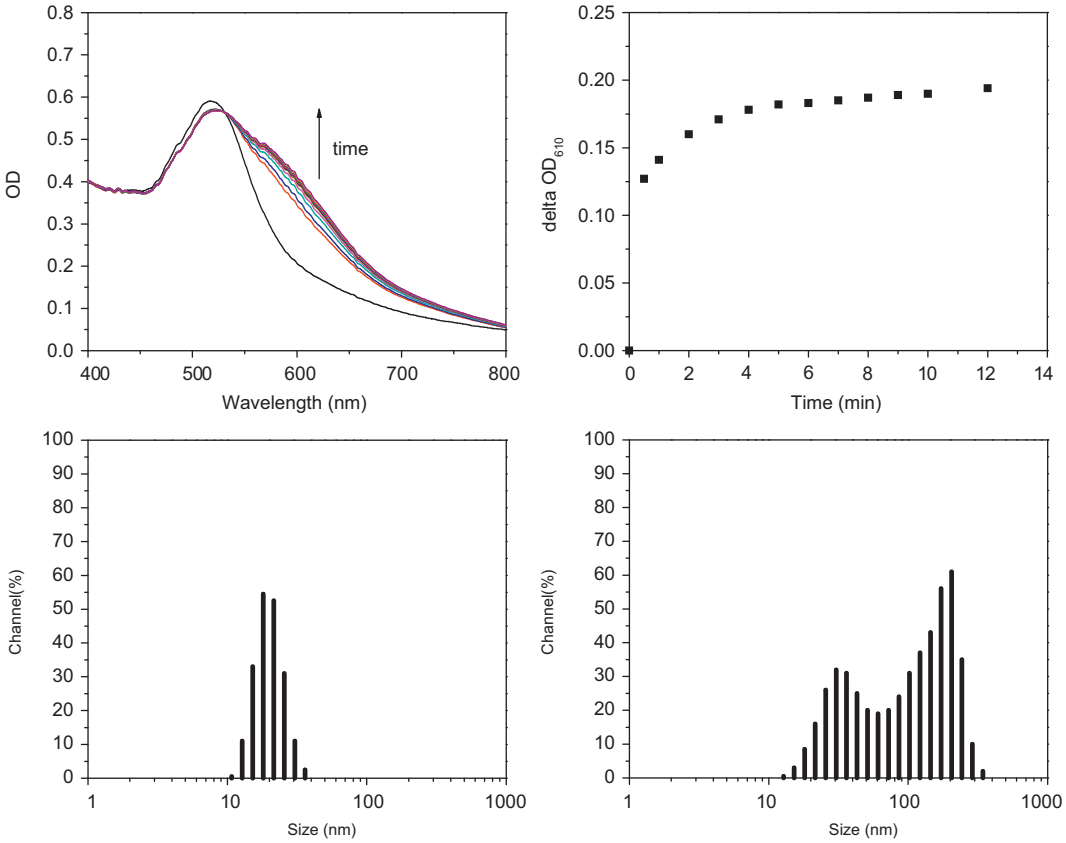

Fig. 3. UV–vis spectra and particle size analysis of SA-AuNPs with virus. UV–vis absorption spectra measured at 0, 0.5, 1, 2, 3, 4, 5, 6, 7, 8, 9, 10 and 12 min after the addition of 1.25 vol% influenza B/Victoria. Overall absorption spectra (A), change of OD_{610} over time (B), particle size analysis results measured before (C) and after (D) addition of 1.25 vol% influenza B/Victoria.

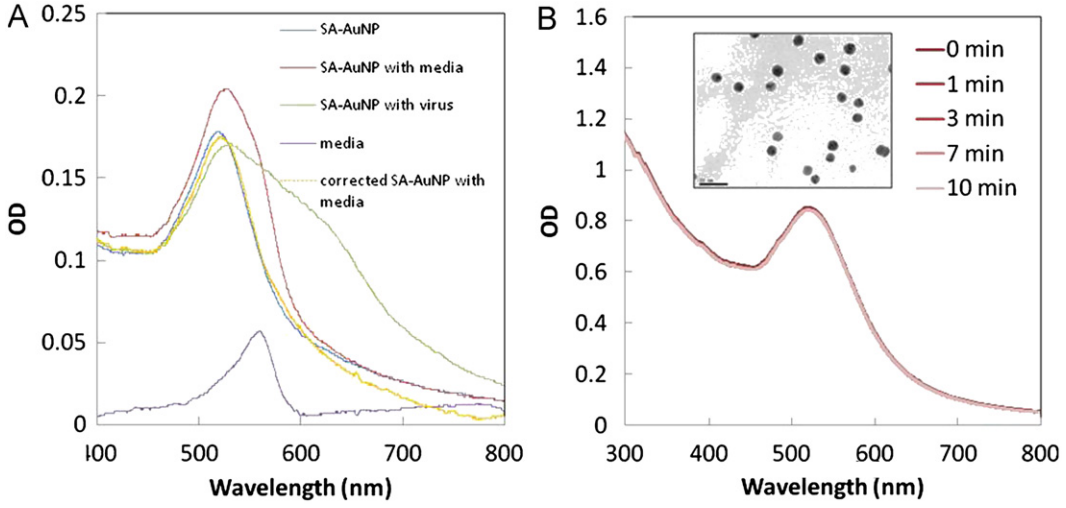

Fig. 4. Absorption spectra of AuNP solution under different conditions: (A) medium present in influenza B/Victoria virus solution was added to SA-AuNP solution and (B) Gelatin-AuNP (20 nm) solution was incubated with 2.5 vol% influenza B/Victoria solution. Inset of B: TEM image of Gelatin-AuNPs, scale bar—50 nm.

matched well with that of SA-AuNPs in water, indicating that the presence of medium does not cause SA-AuNP aggregation. Additionally, the potential for virus binding nonspecifically to nanoparticles and cause aggregation was tested. Gelatin-AuNPs, with similar spherical shape and size distribution (Fig. 4B inset, diameter of ~20 nm by TEM analysis) but lacking sialic acid were assayed for aggregation in the presence of viral particles. No change was observed in either the plasmonic band or the 600–700 nm region. These results suggest that SA-AuNP aggregation is indeed caused by viral particles via the interaction between sialic acid on SA-AuNP surface and hemagglutinin on the viral particle surface.

To further test the hypothesis that the sialic acid on the SA-AuNP is interacting with hemagglutinin, influenza B/Victoria stock solution was pre-incubated with an excess of 1.25 mM sialic acid to thus occupy all hemagglutinin binding sites.

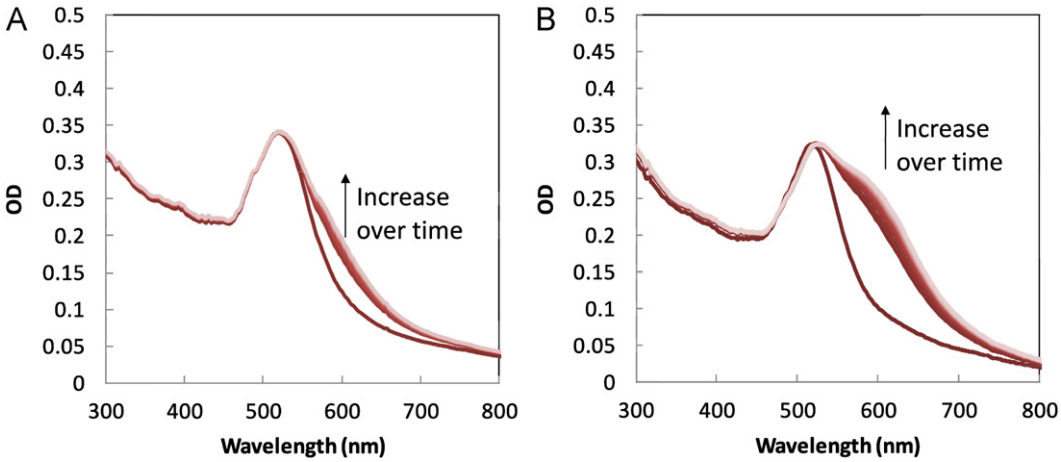

Fig. 5. Effect of SA pre-treatment to virus on the SA-AuNP aggregation, monitored by UV–vis absorption spectroscopy: (A) SA pre-incubated influenza B/Victoria (2.5 vol%) incubated with SA-AuNP (0.4 nM) and (B) untreated influenza B/Victoria (2.5 vol%) with SA-AuNP (0.4 nM).

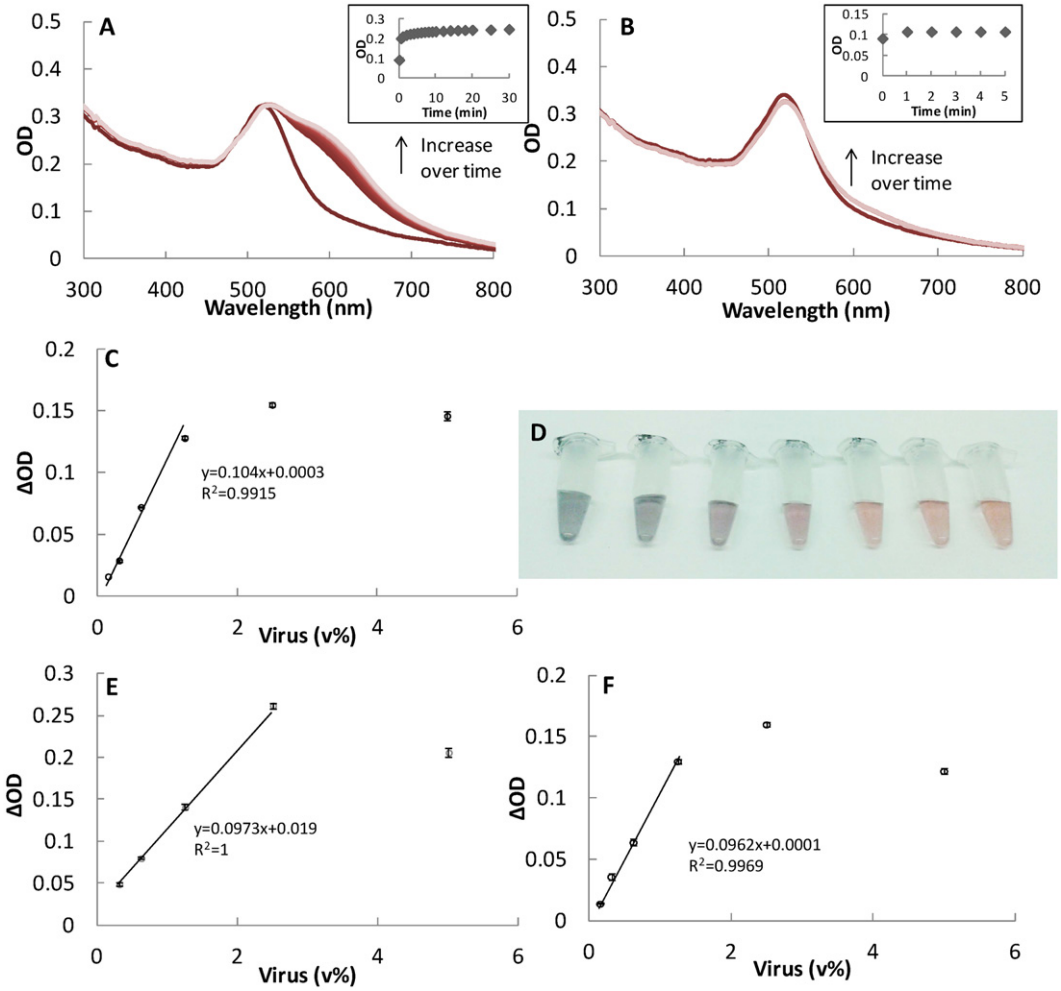

Fig. 6. (A) Absorption spectra of 0.4 nM SA-AuNPs over time after addition of 2.5 vol% influenza B/Victoria solution; inset, OD_{610} value change. (B) Absorption spectra of 0.4 nM SA-AuNPs over time after addition of 0.156 vol% virus solution; inset, change in OD_{610}. (C) Change in OD_{610} value after reaching plateau for different dilutions of virus. A linear correlation is observed for dilutions <1.25 vol% virus. (D) Photograph of SA-AuNPs with different dilutions of virus, 5, 2.5, 1.25, 0.625, 0.3125, 0.156 and 0 vol% from left to right, respectively. (E) Change in OD_{610} measured for 0.8 nM SA-AuNP solution after addition of influenza B/Victoria. A linear correlation is observed for dilutions <2.5 vol% virus. (F) Change in OD_{610} measured for 0.4 nM SA-AuNP solution after addition of influenza B/Yamagata. A linear correlation is observed for dilutions <1.25 vol% virus.

This pre-treated virus solution was then incubated with SA-AuNP solution and aggregation was assayed by changes in absorbance in the UV–vis spectrum. As shown in Fig. 5, a smaller ΔOD ($\sim$3.2 times) was observed with SA pre-treated virus solution as compared to the non-treated virus solution. This suggests that the sialic acid groups on the SA-AuNPs interact with hemagglutinin on virus surface in a similar manner as the free sialic acid in solution.

Different dilutions of influenza B/Victoria were added to 0.4 nM SA-Au NP solution to determine limit of detection. Seven different concentrations of virus solution, 5, 2.5, 1.25, 0.625, 0.3125, 0.156 and 0 vol%, were tested in the colorimetric test. The change in absorbance of SA-AuNPs over time is shown after adding 2.5 vol% virus solution in Fig. 6A and 0.156 vol% in Fig. 6B. A linear correlation is observed between ΔOD and the amount of added virus solution when the virus concentration was below 1.25 vol% (Fig. 6C). While virus solution of 0.156 vol% was readily detected, the detection limit could be estimated to be 0.09 vol%. Note that, from the insets of Fig. 6A and B, it took longer to reach plateau in absorption when a higher titer of virus was added. The final solutions after each test are shown in the photograph (Fig. 6D), illustrating the gradual change from red to purple color as the amount of virus solution increases.

It has been reported that interparticle distance, when larger than 5 times the nanoparticle radius, does not cause electromagnetic coupling between the particles (Ghosh and Pal, 2007). At higher concentrations of virus (e.g. 2.5 and 5 vol%), as ratio of virus to particles increases, the proportion of SA-AuNPs that can be bound to the same viral particle decreases. This results in longer interparticle distance between neighboring SA-AuNPs on the viral particle surface, and less signal. We carried out another set of colorimetric tests using a higher concentration of SA-AuNP solution (0.8 nM), while maintaining the same concentrations of virus solution. The results in Fig. 6E show that the linear range of ΔOD vs. concentration of added virus solution has extended to 2.5 vol% of virus in the solution. This illustrates the importance of having an excessive amount of SA-AuNPs in the starting solution when applying this scheme for virus detection. To validate these results with another virus preparation, influenza B/Yamagata subtype was also tested with 0.4 nM SA-AuNPs solution. The results are similar to those of influenza B/Victoria, and shown in Fig. 6F.

A recent paper by Niikura et al. (2009) has reported the use of gold nanoparticles functionalized by sialic acid-linked lipids to detect virus-like particles. This study included the synthesis of the sialic acid-linked lipid in four complicated steps and subsequent step to finally obtain the sialic acid-functionalized gold nanoparticles for virus-like particle detection. In comparison, our one-pot synthesis of sialic acid-AuNPs is simpler, more economical and environmentally friendly. This report is the first to demonstrate that such colorimetric scheme indeed works for the detection of actual virus.

4. Conclusions

In conclusion, a simple and efficient method to synthesize sialic acid reduced and protected gold nanoparticles was developed. The resulting SA-AuNPs showed very monodisperse spherical shape with a diameter of 20.1 ± 1.8 nm. The SA-AuNPs can readily detect influenza B virus (HA titer of 512) diluted to 0.156 vol% and the upper limit of linearity can be extended to higher virus titer with a more concentrated SA-AuNP solution. The method works for different influenza B lineages (Victoria and Yamagata). Results from control experiments support the hypothesis that sialic acid molecules on SA-AuNP surface interact with viral envelope protein hemagglutinin, causing a colorimetric change of the SA-AuNP solution.

Acknowledgments

Supports from the National Science Foundation (CBET-0931677, CBET-1065633) and National Institute of Health (R01AI089450 from NIH/NIAID to AAW) are gratefully acknowledged.

References

Bouvier, N.M., Palese, P., 2008. Vaccine 26 (Suppl. 4(0)), D49–D53.
Darbha, G.K., Singh, A.K., Rai, U.S., Yu, E., Yu, H., Chandra Ray, P., 2008. Journal of the American Chemical Society 130 (25), 8038–8043.
Elghanian, R., Storhoff, J.J., Mucic, R.C., Letsinger, R.L., Mirkin, C.A., 1997. Science 277 (5329), 1078–1081.
Ghosh, S.K., Pal, T., 2007. Chemical Reviews 107 (11), 4797–4862.
Killian, M.L., 2008. In: Spackman, E. (Ed.), Methods in Molecular Biology, vol. 436: Avian Influenza Virus. Humana Press, Totowa, NJ, pp. 47–52.
Kunkel, F., Herrler, G., 1993. Virology 195 (1), 195–202.
Landry, M.L., 2011. Current Opinion in Pediatrics 23 (1), 91–97.
Mahony, J.B., 2008. Clinical Microbiology Reviews 21 (4), 716–747.
Medley, C.D., Smith, J.E., Tang, Z., Wu, Y., Bamrungsap, S., Tan, W., 2008. Analytical Chemistry 80 (4), 1067–1072.
Niikura, K., Nagakawa, K., Ohtake, N., Suzuki, T., Matsuo, Y., Sawa, H., Ijiro, K., 2009. Bioconjugate Chemistry 20 (10), 1848–1852.
Papp, I., Sieben, C., Ludwig, K., Roskamp, M., Böttcher, C., Schlecht, S., Herrmann, A., Haag, R., 2010. Small 6 (24), 2900–2906.
Pavlov, V., Xiao, Y., Shlyahovsky, B., Willner, I., 2004. Journal of the American Chemical Society 126 (38), 11768–11769.
Salgado, C.D., Farr, B.M., Hall, K.K., Hayden, F.G., 2002. The Lancet: Infectious Diseases 2 (3), 145–155.
Sauter, N.K., Hanson, J.E., Glick, G.D., Brown, J.H., Crowther, R.L., Park, S.J., Skehel, J.J., Wiley, D.C., 1992. Biochemistry 31 (40), 9609–9621.
Storhoff, J.J., Marla, S.S., Bao, P., Hagenow, S., Mehta, H., Lucas, A., Garimella, V., Patno, T., Buckingham, W., Cork, W., Miller, U.R., 2004. Biosensors and Bioelectronics 19 (8), 875–883.
Suzuki, T., Portner, A., Scroggs, R.A., Uchikawa, M., Koyama, N., Matsuo, K., Suzuki, Y., Takimoto, T., 2001. Journal of Virology 75 (10), 4604–4613.
Thompson, W.W., Shay, D.K., Weintraub, E., Brammer, L., Bridges, C.B., Cox, N.J., Fukuda, K., 2004. JAMA: The Journal of the American Medical Association 292 (11), 1333–1340.
Uncapher, C.R., DeWitt, C.M., Colonno, R.J., 1991. Virology 180 (2), 814–817.
Varghese, J.N., Colman, P.M., van Donkelaar, A., Blick, T.J., Sahasrabudhe, A., McKimm-Breschkin, J.L., 1997. Proceedings of the National Academy of Sciences 94 (22), 11808–11812.
Vlasak, R., Luytjes, W., Spaan, W., Palese, P., 1988. Proceedings of the National Academy of Sciences 85 (12), 4526–4529.
Wang, Q., Tian, X., Chen, X., Ma, J., 2007. Proceedings of the National Academy of Sciences 104 (43), 16874–16879.
Weis, W., Brown, J.H., Cusack, S., Paulson, J.C., Skehel, J.J., Wiley, D.C., 1988. Nature 333 (6172), 426–431.
Zhong, Z., Patskovskyy, S., Bouvrette, P., Luong, J.H.T., Gedanken, A., 2004. Journal of Physical Chemistry B 108 (13), 4046–4052.